

UCLA

UCLA Previously Published Works

Title

Deformation of Optic Nerve Head and Peripapillary Tissues by Horizontal Duction

Permalink

<https://escholarship.org/uc/item/3v44v45w>

Journal

American Journal of Ophthalmology, 174

ISSN

0002-9394

Authors

Chang, Melinda Y

Shin, Andrew

Park, Joseph

et al.

Publication Date

2017-02-01

DOI

10.1016/j.ajo.2016.10.001

Peer reviewed



HHS Public Access

Author manuscript

Am J Ophthalmol. Author manuscript; available in PMC 2018 February 14.

Published in final edited form as:

Am J Ophthalmol. 2017 February ; 174: 85–94. doi:10.1016/j.ajo.2016.10.001.

Deformation of Optic Nerve Head and Peripapillary Tissues By Horizontal Duction

Melinda Y. Chang^{1,2}, Andrew Shin^{1,2}, Joseph Park^{1,2}, Aaron Nagiel^{1,2}, Robert A. Lalane^{1,2}, Steven D. Schwartz^{1,2}, and Joseph L. Demer^{1,2,3,4,5}

¹Department of Ophthalmology, David Geffen Medical School at University of California, Los Angeles, U.S.A

²Stein Eye Institute, David Geffen Medical School at University of California, Los Angeles, U.S.A

³Department of Neurology, David Geffen Medical School at University of California, Los Angeles, U.S.A

⁴Neuroscience, David Geffen Medical School at University of California, Los Angeles, U.S.A

⁵Bioengineering Interdepartmental Programs, David Geffen Medical School at University of California, Los Angeles, U.S.A

Abstract

Purpose—To ascertain deformation of the optic nerve head (ONH) and peripapillary tissues caused by horizontal duction.

Design—Prospective, experimental study.

Methods—Optical coherence tomography of the ONH region was performed in 23 eyes of twelve normal volunteers in central gaze and increasing (10, 20, and 30°) adduction and abduction. Main outcome measures were changes from central gaze in the configuration of the ONH and peripapillary tissues in eccentric gazes.

The corresponding author is Joseph L. Demer, M.D., Ph.D. Stein Eye Institute, 100 Stein Plaza, UCLA, Los Angeles, California, 90095-7002 U.S.A. Telephone: 310-825-5931, fax: 310-206-7826, jld@jsei.ucla.edu.

Meeting presentation: Presented at Association for Research in Vision and Ophthalmology, Seattle, WA, May 4, 2016.

Financial Disclosures:

1. Melinda Chang: No financial disclosures
2. Andrew Shin: No financial disclosures
3. Joseph Park: No financial disclosures
4. Aaron Nagiel: No financial disclosures
5. Robert Lalane: No financial disclosures
6. Steven Schwartz: In regards to the work under consideration, Dr. Schwartz does not have any relevant conflicts of interest. Outside of the submitted work, Dr. Schwartz reports grants from Genentech (South San Francisco, CA), grants from Optos (Marlborough, MA), others from Avalanche (Menlo Park, CA), and grants from Ocata Therapeutics (Marlborough, MA).
7. Joseph Demer: No financial disclosures.

Results—Adduction but not abduction was associated with significant, progressive relative posterior displacement of the temporal peripapillary retinal pigment epithelium (tRPE) from its position in central gaze reaching $49 \pm 10 \mu\text{m}$ in 30° adduction (standard error of mean, $p < 0.0001$). Absolute (anterior or posterior) optic cup displacement (OCD) averaged $41 \pm 7 \mu\text{m}$ in 30° adduction. Linear regression showed significant effect of adduction on absolute OCD (slope $1.09 \pm 0.36 \mu\text{m}/\text{degree}$, $p = 0.0037$). In 20° and 30° adduction, all eyes exhibited significant progressive temporal ONH tilting reaching $3.1 \pm 0.4^\circ$ in 30° adduction ($p < 0.0001$). Abduction was not associated with significant peripapillary RPE displacement, OCD, or ONH tilt. Both nasal and temporal peripapillary choroid averaged 9 to $19 \mu\text{m}$ thinner in adduction and abduction than in central gaze ($p < 0.02$).

Conclusions—Adduction temporally tilts and displaces the prelaminar ONH and peripapillary tissues. Both adduction and abduction compress the peripapillary choroid. These effects support MRI and biomechanical evidence that adduction imposes strain on the ONH and peripapillary tissues. Repetitive strain from eye movements over decades might in susceptible individuals lead to optic neuropathies such as normal tension glaucoma.

Graphical abstract

Optical coherence tomography confirms biomechanical predictions of optic cup and temporal peripapillary deformation due to optic nerve sheath traction in adduction but not abduction. These effects support magnetic resonance imaging and biomechanical evidence that adduction imposes strain on the optic nerve head and peripapillary tissues. Repetitive strain from eye movements over decades might in susceptible individuals lead to optic neuropathies such as normal tension glaucoma via a novel, intraocular pressure-independent mechanism of optic nerve damage.

Introduction

Recent evidence from biomechanical models suggests that optic nerve damage, such as occurs in glaucoma, may result from mechanical factors in addition to elevated intraocular pressure (IOP).¹⁻⁴ These models indicate that optic neuropathy may result from stress (force/cross sectional area) and strain (local deformation induced by applied stress) on the load-bearing tissues of the optic nerve head (ONH) such as the peripapillary sclera, lamina cribrosa, and scleral canal wall.¹ While elevated IOP probably contributes to this damage,⁵ other factors must also be implicated given the high prevalence of glaucoma at normal or subnormal IOP.⁶ Normal tension glaucoma accounts for 40% of glaucoma in the Netherlands and up to 94% of glaucoma in Asian populations,⁷⁻¹¹ depending upon the definition of ‘normal’ IOP. However, statistically ‘normal’ IOP in some Asian populations may be slightly greater than accepted in Caucasians, having been recently reported to be $17-18 \pm \sim 3 \text{ mmHg}$ (SD) in 5,919 Chinese children.¹² The factors beyond elevated IOP that contribute to optic nerve (ON) damage remain poorly understood.⁶

To date, biomechanical models have considered the structural properties of laminar and peripapillary tissues, in addition to elevated IOP, as factors that may cause thinning of prelaminar tissues and laminar deformation as observed in optic neuropathies, particularly glaucoma.^{1, 2, 5} Herein we consider a novel factor that may contribute to optic neuropathy – namely, ocular rotation, particularly adduction.

A recent study utilizing magnetic resonance imaging (MRI) showed that the ON sheath becomes tethered in adduction, but not abduction.¹³ Another recent study using finite element analysis predicted that horizontal duction causes ONH strain.¹⁴ Substantial see-saw movements of the peripapillary tissues have been demonstrated by optical coherence tomography (OCT) during large horizontal ductions in patients with ONH swelling caused by elevated intracranial pressure in papilledema, but not associated with ONH swelling due to anterior ischemic optic neuropathy.¹⁵ We sought confirmation of these findings using in vivo imaging of the human ONH and peripapillary tissues with OCT during a graded range of horizontal ductions.

Biomechanical effects on the ONH of both severe, acute IOP elevation, and papilledema have been examined by OCT.¹⁶⁻²⁰ Other studies have investigated the OCT changes resulting from IOP decrease by trabeculectomy, and decreased cerebrospinal fluid (CSF) pressure by lumbar puncture, CSF shunting, and medical therapy.^{21, 22} The peripapillary retinal pigment epithelium (RPE) was used as a reference point in these OCT studies because it is easily identifiable and approximates the shape of the load-bearing sclera.^{18, 20, 22} These studies have shown that OCT can reliably image peripapillary and prelaminar tissues.^{17, 18} Moreover, OCT can be used to distinguish these pathological optic neuropathies from normal ONs and demonstrate effects of IOP-lowering treatment on the ONH and peripapillary tissues.^{21, 22}

Since MRI demonstrates marked tethering and sometimes even globe retraction in adduction when the ON sheath becomes taut, we hypothesized that this phenomenon might cause progressive shape changes in peripapillary and prelaminar ONH tissues demonstrable by OCT that are specific to adduction. We also supposed that these effects might alter choroidal thickness. The current study was performed to test these predictions.

Methods

Subjects

This study was approved by the Institutional Review Board of the University of California, Los Angeles, and conformed to the requirements of the U.S. Health Insurance Portability and Accountability Act. Twelve volunteers of average age 21 ± 0.7 (standard deviation, SD, range 19 - 22) years with no ocular abnormalities except refractive error were recruited and gave written informed consent prior to participation. Complete ophthalmic history and examination were performed to exclude ocular pathology. All eyes had intraocular pressure < 21 mmHg and no evidence of glaucomatous optic neuropathy. Mean spherical equivalent of manifest refractive error was -2.6 ± 2.2 (range plano to -5) diopters. One eye was excluded due to incomplete data collection in eccentric gazes, so data from 23 eyes were analyzed.

OCT Acquisition

After pupillary dilation with topical phenylephrine 2.5%, subjects were imaged using spectral-domain OCT (RS-3000, Nidek Co., Ltd., Japan). First, macula line and retinal nerve fiber scans were performed in each eye, to verify absence of macular and ONH pathology. Volume scans of the ONH were then sequentially performed first in the right and then left

eye in central gaze, increasing adduction (10, 20, and 30°), and increasing abduction (10, 20, and 30°). Finally, in four subjects, ONH volume scans were repeated in central gaze to assess measurement repeatability. Horizontal duction was accomplished by head rotation in the scanner by the desired angle measured using a goniometer. Each OCT volume acquisition comprised 128 horizontal B-scans covering a 9 mm wide and 4.2 mm high region centered on the ONH. After the initial scan in central gaze, the scanning laser ophthalmoscope auto-tracking “follow-up” function was used to ensure that the line scans of the disc were in registration for subsequent scans. The auto-tracking function uses anatomical landmarks such as blood vessels to align follow-up scans in precisely the same position as the initial scan, accounting for horizontal, vertical, and torsional shifts that may occur with eccentric gaze and change in patient positioning. Vertex distance from the scanner to the eye was adjusted by caliper to be constant to avoid magnification changes.

OCT Analysis

Images were analyzed using the programs NIH *ImageJ64* (W. Rasband, National Institutes of Health, Bethesda, MD, USA; <http://rsb.info.nih.gov/ij/>, 1997–2009 [in the public domain]) and *Adobe Photoshop* (Adobe Systems Inc., San Jose, CA). Image aspect ratio was corrected in *ImageJ64*. From the 128 line scans in primary gaze, the scan representing the center of the ONH was selected. Use of the auto-tracking function allowed for identification of corresponding scans in primary and eccentric gaze positions. Using layers and reduced opacity in *Photoshop*, the corresponding scans in each eccentric gaze position were superimposed in different color on the primary gaze ONH scan after rotation and translation to superimpose the position and angulation of the far nasal periphery as the reference structure. Scans were superimposed along the RPE starting at the far nasal periphery of the images, approximately 4 mm nasal to the ONH. Superimposition continued for at least 2.5 mm along the nasal RPE toward the ONH, to ensure that eccentric gaze scans were rotationally aligned with respect to central gaze. The far nasal periphery was chosen as reference structure based on preliminary analysis of initial scans, in which alignment was evaluated relative to both the nasal vs. alternatively the temporal periphery. Using the two alternative alignment references, results were identical in magnitude, but opposite in direction, as demonstrated in Fig. 1. The nasal periphery was therefore selected as the reference point for subsequent scans because prior MRI and biomechanical studies suggested that the effect of ocular ductions on peripapillary tissues is greatest temporally.

For each eccentric scan, the following parameters were measured relative to central gaze: displacement of the optic cup (Figs. 1 and 2); posterior displacement of the temporal peripapillary retinal pigment epithelium (tRPE, Fig. 1); anterior displacement of the nasal peripapillary RPE (nRPE, Fig. 2); and change in ONH angle, measured as that of a line connecting the peripapillary nasal and temporal RPE surfaces immediately adjacent to the ONH (Figs. 1 and 2). Temporal ONH tilting was designated positive, and nasal tilting negative. In eccentric and central gazes, we measured the thickness of the choroid 1 mm nasal to the nasal junction of the RPE and ONH, and 0.3 mm temporal to the temporal junction of the RPE and ONH (Fig. 1). These sites for choroidal thickness measurements were the nearest ones from the ONH at which the choroid was clearly present in most scans.

Statistical analysis

Since this is a study of normal physiology, the individual eye was taken to be the unit of analysis.^{23, 24} To exclude the possibility that correlation between the two eyes of each subject might exaggerate the statistical significance of differences, we repeated statistical analyses using a generalized estimating equation (GEE) model to account for interocular correlations within subjects using *SPSS* (IBM Corporation, Armonk, NY). Optic cup displacement, tRPE posterior displacement, nRPE anterior displacement, and change in ONH angle were compared with primary gaze using one-sample t-tests against the null hypothesis of zero change. Nasal and temporal choroidal thickness in each eccentric gaze position and in repeated central gaze were compared to initial primary gaze using two-tailed paired t-tests. Linear regression analysis was performed for each measure. The 0.05 level was considered statistically significant.

Results

Progressive ocular duction was associated with progressive changes in relative ONH configuration, as well as peripapillary RPE displacement. Figure 1 illustrates the typical changes in large angle adduction. Because the field of view of the OCT images was limited to only 9 mm, it was only possible to interpret relative position changes within this region, or to interpret changes relative to any absolute reference such as the center of the globe. For purposes of analysis, two different relative reference points were chosen that were as distant as possible from the presumed site of greatest deformation at the ONH. When the most nasal RPE was used as the reference for alignment of scans in central gaze (red), adduction (green) resulted in posterior displacement of the optic cup and temporal peripapillary RPE (tRPE) with only minimal displacement of the nasal peripapillary RPE (nRPE) (Fig. 1A, B). With the scans alternatively aligned on the most temporal RPE, the optic cup shifted in adduction by the same magnitude, but in the opposite direction (Fig. 1C, D). Use of a temporal alignment reference resulted in apparent anterior shift of the nRPE in adduction, by the same distance but in the opposite direction as tRPE displacement interpreted using nasal alignment of scans (Fig. 1A-D). Thus, both nasal and temporal alignment resulted in the same degree of relative temporal tilting of the ONH in adduction (Fig. 1A-D), and the same magnitude of deformation of the optic cup and peripapillary tissues in adduction, but opposite in direction. Since a single reference structure must be chosen for consistency, we elected to align scans using the far nasal periphery, and all further analyses are reported relative to this structure.

Although the nRPE was minimally displaced during adduction in most eyes, five eyes of five subjects demonstrated nasal “buckling” of the peripapillary tissues in adduction, consisting of sharply angulated anterior displacement immediately adjacent to the nasal ONH border, as illustrated in Figure 2. Nasal buckling was typically associated with minimal posterior tRPE displacement (Fig. 2), and was always unioocular. Subjects with nasal buckling did not differ from others in age, sex, refractive error, or intraocular pressure. Nasal buckling resulted in anterior shift of the optic cup and temporal tilting of the ONH in adduction (Fig. 2).

The effects of adduction on optic cup displacement (OCD), tRPE and nRPE shift, and ONH tilt increased progressively with adduction angle. Abduction was associated with slight anterior shift of the tRPE, nRPE, and optic cup, with minimal ONH tilting (Fig. 3), none of which depended significantly on abduction angle.

Temporal peripapillary RPE posterior displacement

The temporal peripapillary RPE shifted progressively posteriorly with increasing adduction (Fig. 4A). In 30° adduction, tRPE was $49 \pm 10 \mu\text{m}$ (mean \pm SEM) farther posterior than in central gaze. In abduction, there was no significant tRPE displacement. Linear regression indicated a significant effect of adduction (linear regression coefficient of determination 0.22, $p < 0.0001$, GEE analysis $p = 0.000$) but not abduction on tRPE displacement (Fig 4B). The slope of the linear relationship for adduction was 2.18 ± 0.50 , indicating that the temporal peripapillary RPE shifted posteriorly on average by approximately $2 \mu\text{m}$ per degree. In abduction, the regression slope did not significantly differ from zero.

Nasal peripapillary RPE anterior displacement

Although most eyes exhibited no significant shift of the nRPE during horizontal duction, some eyes exhibited the phenomenon of nasal “buckling” consisting of sharply angulated anterior displacement of the nasal peripapillary tissues (Fig. 2). This phenomenon is quantitatively evident in the Figure 4B plot of nRPE anterior displacement from primary gaze during horizontal duction. Large inter individual variability in nRPE displacement that ranged from 0 to $140 \mu\text{m}$ in 30° adduction was driven by only five eyes, while the remaining eyes exhibited almost no nRPE displacement (Fig. 4B). Eyes exhibiting nasal buckling averaged less posterior displacement of the tRPE than did eyes without nasal buckling. Linear regression demonstrated significant effect of adduction (linear coefficient of determination 0.11, $p = 0.0062$, GEE analysis $p = 0.004$) but not abduction ($p = 0.74$) on nRPE displacement (Fig. 4B). The linear regression slope for adduction was $1.14 \pm 0.40 \mu\text{m}$ per degree, indicating that the nRPE was anteriorly displaced on average by $1 \mu\text{m}$ per degree adduction.

Optic cup displacement (OCD) in eccentric gazes varied widely, particularly in adduction. For example, in 30° adduction OCD ranged between $94 \mu\text{m}$ anterior and $132 \mu\text{m}$ posterior displacement. Review of the OCTs showed that OCD was anterior when nRPE anterior displacement exceeded tRPE posterior displacement, and posterior when tRPE posterior displacement exceeded nRPE anterior displacement (Figs. 1 and 2). Therefore, the OCD direction depended on the predominance of nasal vs. temporal peripapillary deformation. For this reason, we analyzed the absolute value of OCD in either direction. Absolute OCD averaged $41 \pm 7 \mu\text{m}$ in 30° adduction. Linear regression of absolute OCD showed significant relationship to adduction ($p = 0.0037$, GEE analysis $p = 0.014$) but not abduction (Fig. 5A). In adduction, the coefficient of determination was 0.13, and the regression slope was $1.09 \pm 0.36 \mu\text{m/degree}$. In other words, the optic cup was displaced $1 \mu\text{m}$ anteriorly or posteriorly for each degree adduction.

Change in ONH Angle (temporal tilting)

Mean angle of temporal ONH tilting in eccentric gaze positions relative to central gaze is displayed in Fig.5B. In 20° and 30° adduction, the ONH tilted temporally in all eyes. At 30° adduction, the ONH tilted temporally $3.1 \pm 0.4^\circ$, but there was no significant tilting in abduction. Linear regression showed a significant effect of adduction (coefficient of determination 0.35, $p < 0.0001$, GEE analysis $p = 0.000$) but not abduction on ONH tilt. The regression slope in adduction was $0.12 \pm 0.02^\circ/\text{degree}$, indicating that the ONH tilted temporally by approximately 0.1° per degree, in other words 1° for each 10° adduction.

Choroidal thickness

The nasal and temporal choroids significantly thinned in both adduction and abduction relative to central gaze (Table 1). Low image quality precluded measurement of the nasal choroid in 3 eyes, and the temporal choroid in 9 eyes. In central gaze, nasal choroidal thickness was $247 \pm 10 \mu\text{m}$. The nasal choroid was significantly thinned in all eccentric horizontal gaze positions, with averages ranging from 228 to 235 μm ($p < 0.002$). Temporal choroidal thickness in central gaze was $184 \pm 9 \mu\text{m}$, and was also significantly thinned in all eccentric horizontal gaze positions, with mean thickness ranging from 166 to 175 μm ($p < 0.03$).

Reproducibility

Replication analysis demonstrated absence of significant change in tRPE position in central gaze at the end of the sequence of scans compared to the initial scan in the same position (mean anterior displacement $5 \pm 3 \mu\text{m}$, $p = 0.14$). Other measurements repeated in central gaze at the end of the sequence demonstrated similarly high repeatability, with neither significant displacement of nRPE and optic cup, nor significant change in ONH angle and nasal and temporal choroidal thickness compared to initial measurements ($P > 0.05$). This repeatability supports the interpretation that observed changes were due to duction angle.

Discussion

The present study provides novel OCT evidence that horizontal ocular ductions substantially deform the prelaminar ONH and peripapillary tissues over such a wide extent that even wide field imaging cannot delineate the full spatial limits of deformation. This deformation results in relative posterior positioning of the temporal peripapillary tissues compared with anterior positioning of the nasal tissues in adduction. Based upon published evidence that the optic nerve sheath selectively exerts posterior traction on the temporal ONH and peripapillary tissues in adduction, we have chosen to report the OCT data relative to a reference at the nasal periphery, under the assumption that resulting deformation of ocular tissues would be least in that location. Using this reference, adduction caused temporal ONH tilting with displacement of the optic cup and nasal and temporal peripapillary RPE, but abduction did not. Both adduction and abduction compressed the nasal and temporal peripapillary choroid.

The foregoing mechanical changes in the prelaminar ONH and peripapillary tissues are likely to be due to ON sheath traction. Recent MRI studies revealed that the ON is insufficiently long to permit full, unhindered adduction.¹³ Thus the globe is tethered during

large angle adduction, where the temporal ON sheath is straightened and flattened against the temporal side of the ON, and its resulting elastic tension is concentrated at the temporal edge of the ON's scleral canal.¹³ Finite element analysis biomechanical modeling predicts high strains in the ONH during horizontal duction.¹⁴ MRI suggests that the high tensile strain on the temporal peripapillary tissues during adduction occurs in the same region as peripapillary atrophy that is typically located temporally²⁵ and commonly seen in myopia²⁶ and glaucoma,²⁷ where the location of peripapillary atrophy correlates with topography²⁸ and visual field loss.²⁹ These peripapillary changes are also associated with temporally located posterior staphylomata and chorioretinal atrophy in high myopia,³⁰ a condition in which MRI shows foreshortening of the ON and particularly striking ON sheath tethering and even globe retraction in adduction.¹³

In adduction by some eyes, the tRPE was minimally displaced, while the immediate nRPE was sharply angulated anteriorly, a phenomenon we term “nasal buckling” (Fig. 2). MRI shows that when the temporal ON sheath is flattened during adduction, cerebrospinal fluid (CSF) is redistributed to the nasal side of the ON, and the globe often retracts slightly into the orbit. It is possible that rigidity of the straightened ON sheath under normal CSF pressure could force the peripapillary tissues anteriorly in some eyes, similar to reported in central gaze in patients with elevated intracranial pressure.^{18, 20} Action of CSF pressure on the lamina cribrosa has been previously considered, with some authors postulating that glaucoma may be related to the difference between CSF pressure and IOP, rather than IOP alone.³¹

Although the optic cup shifted posteriorly during adduction in most eyes, nasal buckling caused anterior shift instead in a minority of eyes. Absolute OCD in 30° adduction was $41 \pm 7 \mu\text{m}$, which is at least as great as the optic cup deepening observed on OCT after severe, acute IOP elevation.¹⁶ Jiang et al performed optic nerve OCT before and after a dark room prone provocation of acute primary angle closure glaucoma suspects. Overall, the mean IOP elevation in acute primary angle closure was 10 mmHg, but there was no change in OCD. However, among eyes with 32 mmHg mean IOP elevation, the optic cup deepened an average of only 35 μm .¹⁶

The ONH tilted temporally in all eyes during 20° and 30° adduction. Temporal ONH tilt is associated with glaucoma³² and myopia,^{30, 33} and is typical of the Asian population,³⁴ in which the majority of glaucoma occurs at a normal IOP.^{10, 11, 35} Park *et al.* reported temporal ONH tilt in 46% of eyes with myopic normal tension glaucoma.³² Despite the high prevalence of ONH tilt, the cause of tilting has been obscure. Occasional cases of tilted optic discs are believed to be congenital,³⁶ but in most cases ONH tilt is progressive over time, particularly in myopic eyes.³⁷ Kim *et al.* followed children using serial disc photography, and found that there was progressive temporal ONH tilt and peripapillary atrophy in 43% of eyes, associated with myopic shift.³⁷ The authors theorized that this association occurred due to scleral stretching in myopic eyes, but their theory fails to explain the temporal preponderance of the phenomena. Moreover, myopia did not account for all cases of ONH tilting. In conjunction with MRI evidence,¹³ the present OCT findings suggest that ON sheath traction on the temporal peripapillary sclera in adduction may be a principal cause of temporal ONH tilt. Although reversible ONH tilting was observed here in adduction, over

time this might cause permanent ONH tilt by remodeling of the ONH and peripapillary tissues. Given that the extraocular muscle force associated with initiation of dynamic saccades far exceeds that of maintaining static eccentric gaze,³⁸ chronic remodeling of ONH and peripapillary tissues is more likely to be related to saccadic eye movements, rather than prolonged eccentric gaze such as occurs in strabismus.

The nasal and temporal peripapillary choroid were significantly thinned in all eccentric horizontal gaze positions studied here. Compression of prelaminar tissues during IOP elevation has been reported previously in both humans and animals;^{16, 17, 19, 39} however, choroidal thinning has not previously been examined. We chose to measure choroidal thickness as a possible indicator of mechanical stress. Choroidal thinning in eccentric gazes averaged between 9 and 19 μm (Table 1). For comparison, Jiang et al reported prelaminar tissue thinning of 17 to 18 μm in eyes experiencing on average 32 mmHg acute IOP elevation,¹⁶ while Lee *et al.* found that trabeculectomy increased prelaminar tissue thickness by 6 μm .⁴⁰ Since the deformation of prelaminar and peripapillary tissues during eccentric gaze is comparable to that induced by severe, acute IOP elevation, it is possible that repetitive ocular ductions could eventually cause permanent prelaminar tissue compression and resultant optic neuropathy.

The idea that eye movements may transiently strain the ONH and peripapillary tissues is not really novel, dating back to Purkinje and Helmholtz, who in 1823 and 1911, respectively, described gaze-evoked phosphenes emanating from the physiological cecum.⁴¹ Friedman geometrically deduced that extreme horizontal ductions result in ON traction and peripapillary tissue deformation,⁴² consistent with OCT findings reported here. Purkinje, Helmholtz, and Friedman all reported that the findings were more prominent with adduction and convergence than abduction.^{41, 43} More recently, Wang et al. performed biomechanical modeling with finite element analysis, predicting that ONH strain caused by horizontal eye movements exceeds the strain induced by IOP elevation to 50 mmHg.¹⁴ Finally, Sibony reported prominent horizontal gaze-evoked deformation of the peripapillary basement membrane layer on OCT in eyes with papilledema.¹⁵ These gaze-evoked changes were reversible with CSF pressure reduction, and also occurred to a lesser extent in normal eyes and those with anterior ischemic optic neuropathy. The present study expands on these findings by reporting progressive, duction-induced changes to the prelaminar ONH and peripapillary choroid, in addition to the peripapillary basement membrane position, in normal eyes.

Further experiments are required to determine whether the gaze-induced transient deformations of the prelaminar ONH and peripapillary tissues could, over the long term, permanently damage these tissues. However, the entity of repetitive strain injury, which in cases such as carpal tunnel syndrome leads to neuropathy, is well established.⁴⁴ Furthermore, the risk of repetitive strain injury is related to the frequency and force, as well as the total duration, of the repeated movement.⁴⁴ Snook *et al.* found that repetitive motion injury occurs with wrist extension frequency of 15 motions per minute and 15 N of force, when performed 7 hours per day over a course of 3 weeks.⁴⁵ The mean frequency of saccades is 3 per second (or 180 per minute),⁴⁶ with an estimated total of 183,000 saccades per day.⁴⁷ Saccadic movements are performed throughout the day and even at night during

rapid eye movement sleep.⁴⁸ The force generated by saccades is estimated to be between 0.5 to 1.8 N,⁴⁹ but when the ON sheath is tethered, this force is almost entirely applied to the peripapillary region.¹³ Thus, although the force generated by adducting saccades is relatively small, it is directly applied via the ON sheath to the ONH region, and the frequency and total number of saccades over a lifetime far exceeds those of other movements known to cause repetitive motion injury. Additionally, stress induced in ocular tissues by saccades may increase with age. Mathematical modeling suggests that dynamic saccades produce a traveling stress wave that propagates along the ocular tissues toward the ON and rebounds repeatedly until dampened by structures such as the vitreous gel.⁴⁹ As the vitreous detaches from the eye wall in the aging eye, this damping effect will be decreased, which could increase the stress exerted on the ONH and peripapillary tissues during ductions.

Limitations

This was an exploratory study of the possibility that ocular ductions in normal people might influence morphology of the prelaminar ONH and peripapillary tissues, so the number of subjects was relatively small. Eccentric gaze OCTs were registered to central gaze using the image periphery as a baseline reference, with preference for the nasal periphery on theoretical grounds. Our initial analysis indicated that assigning the temporal periphery as the reference point would have yielded identical results, but in the opposite direction (Fig. 1). Therefore, our results must be interpreted with the understanding that the direction of findings is relative to the reference point chosen, although the magnitude of deformation is probably independent of this choice of reference. We cannot exclude the possibility that the biomechanical effects of duction might be so spatially extensive that even the nasal periphery of the scans were deformed during ductions. We used wide 9 mm OCT dimensions to minimize possible underestimation of effects due to widespread globe deformation, but the OCT analysis can at best characterize only local displacements within this region, and for example would miss uniform or nearly uniform displacement of the entire region imaged. The possible widespread deformation and translation of the globe would if anything cause under-, rather than over-estimation, of mechanical effects of ocular duction on the shape of the prelaminar ONH and peripapillary sclera. In this sense the current high resolution but spatially limited OCT data complement the lower resolution but spatially extensive MRI data¹³ that together confirm both focal and widespread mechanical strain on the posterior eye in adduction. While significant on high resolution OCT having several micron isotropic resolution, the ocular deformations reported here are well below the threshold of detection for even surface coil MRI, where images average over 2 mm plane thickness and typically have 312 micron resolution within planes.⁵⁰

The present OCT scans were limited in depth of penetration because of the increased distance from the scanner necessitated by head rotation and maintenance of constant vertex distance. This prevented imaging the full depth of the lamina cribrosa, and precluded accurate measurement of choroidal thickness in some eyes. Because image quality and frequent peripapillary atrophy prevented us from assessing choroidal thickness immediately adjacent to the ONH, we performed measurements 0.3 and 1 mm from the ONH (temporally and nasally, respectively); these chosen values may not be representative of the effect of

ocular duction immediately adjacent to the ONH in those subjects having closer choroidal proximity to the ONH.

Conclusion

In conclusion, adduction causes significant temporal tilting and displacement of the prelaminar ONH, posterior displacement of the temporal peripapillary tissues, and in some cases a sharply angulated anterior shift of the nasal peripapillary tissues termed “nasal buckling.” These effects are at least as large as those reported in association with acute, extreme IOP elevation. Both adduction and abduction thin the peripapillary choroid. These observations confirm and extend evidence that adduction mechanically strains the ON and peripapillary tissues, supporting the proposition that numerous eye movements over decades might in susceptible individuals cause repetitive strain injury to the ON leading to IOP-independent damage in optic neuropathies such as normal tension glaucoma. Further studies involving patients with optic neuropathies are warranted to test this hypothesis.

Acknowledgments

Funding/Support: This study was supported by grants to Joseph L. Demer from the U.S. Public Health Service, National Institutes of Health (Bethesda, MD), grants EY008313 and EY000331, and an unrestricted grant from Research to Prevent Blindness (New York, NY). The funding organization had no role in the design or conduct of this research.

Other Acknowledgments: None.

References

1. Burgoyne CF, Downs JC. Premise and prediction-how optic nerve head biomechanics underlies the susceptibility and clinical behavior of the aged optic nerve head. *J Glaucoma*. 2008; 17(4):318–28. [PubMed: 18552618]
2. Burgoyne CF, Downs JC, Bellezza AJ, Suh JK, Hart RT. The optic nerve head as a biomechanical structure: a new paradigm for understanding the role of IOP-related stress and strain in the pathophysiology of glaucomatous optic nerve head damage. *Prog Retin Eye Res*. 2005; 24(1):39–73. [PubMed: 1555526]
3. Yang H, Downs JC, Bellezza A, Thompson H, Burgoyne CF. 3-D histomorphometry of the normal and early glaucomatous monkey optic nerve head: prelaminar neural tissues and cupping. *Invest Ophthalmol Vis Sci*. 2007; 48(11):5068–84. [PubMed: 17962459]
4. Yang H, Downs JC, Girkin C, et al. 3-D histomorphometry of the normal and early glaucomatous monkey optic nerve head: lamina cribrosa and peripapillary scleral position and thickness. *Invest Ophthalmol Vis Sci*. 2007; 48(10):4597–607. [PubMed: 17898283]
5. Bellezza AJ, Hart RT, Burgoyne CF. The optic nerve head as a biomechanical structure: initial finite element modeling. *Invest Ophthalmol Vis Sci*. 2000; 41(10):2991–3000. [PubMed: 10967056]
6. Mudumbai RC. Clinical update on normal tension glaucoma. *Semin Ophthalmol*. 2013; 28(3):173–9. [PubMed: 23697620]
7. Sommer A, Tielsch JM, Katz J, et al. Relationship between intraocular pressure and primary open angle glaucoma among white and black Americans. The Baltimore Eye Survey *Arch Ophthalmol*. 1991; 109(8):1090–5. [PubMed: 1867550]
8. Jiang X, Varma R, Wu S, et al. Baseline risk factors that predict the development of open-angle glaucoma in a population: the Los Angeles Latino Eye Study. *Ophthalmology*. 2012; 119(11):2245–53. [PubMed: 22796305]
9. Dielemans I, Vingerling JR, Wolfs RC, Hofman A, Grobbee DE, de Jong PT. The prevalence of primary open-angle glaucoma in a population-based study in The Netherlands. The Rotterdam Study *Ophthalmology*. 1994; 101(11):1851–5. [PubMed: 7800368]

10. Iwase A, Suzuki Y, Araie M, et al. The prevalence of primary open-angle glaucoma in Japanese: the Tajimi Study. *Ophthalmology*. 2004; 111(9):1641–8. [PubMed: 15350316]
11. Kim JH, Kang SY, Kim NR, et al. Prevalence and characteristics of glaucoma among Korean adults. *Korean J Ophthalmol*. 2011; 25(2):110–5. [PubMed: 21461223]
12. Jiang WJ, Wu JF, Hu YY, et al. Intraocular pressure and associated factors in children: the Shandong children eye study. *Invest Ophthalmol Vis Sci*. 2014; 55(7):4128–34. [PubMed: 24876285]
13. Demer J. Optic nerve sheath as a novel mechanical load on the globe in ocular duction. *Invest Ophthalmol Vis Sci*. 2016; 57(4):1826–1838. [PubMed: 27082297]
14. Wang X, Rumpel H, Lim WE, et al. Finite element analysis predicts large optic nerve head strains during horizontal eye movements. *Invest Ophthalmol Vis Sci*. 2016; 57(6):2452–62. [PubMed: 27149695]
15. Sibony P. Gaze evoked deformations of the peripapillary retina in papilledema and ischemic optic neuropathy. *Invest Ophthalmol Vis Sci*. 2016 In Press.
16. Jiang R, Xu L, Liu X, Chen JD, Jonas JB, Wang YX. Optic nerve head changes after short-term intraocular pressure elevation in acute primary angle-closure suspects. *Ophthalmology*. 2015; 122(4):730–7. [PubMed: 25556115]
17. Strouthidis NG, Fortune B, Yang H, Sigal IA, Burgoyne CF. Effect of acute intraocular pressure elevation on the monkey optic nerve head as detected by spectral domain optical coherence tomography. *Invest Ophthalmol Vis Sci*. 2011; 52(13):9431–7. [PubMed: 22058335]
18. Kupersmith MJ, Sibony P, Mandel G, Durbin M, Kardon RH. Optical coherence tomography of the swollen optic nerve head: deformation of the peripapillary retinal pigment epithelium layer in papilledema. *Invest Ophthalmol Vis Sci*. 2011; 52(9):6558–64. [PubMed: 21705690]
19. Agoumi Y, Sharpe GP, Hutchison DM, Nicoleta MT, Artes PH, Chauhan BC. Lamellar and prelaminar tissue displacement during intraocular pressure elevation in glaucoma patients and healthy controls. *Ophthalmology*. 2011; 118(1):52–9. [PubMed: 20656352]
20. Sibony P, Kupersmith MJ, Rohlf FJ. Shape analysis of the peripapillary RPE layer in papilledema and ischemic optic neuropathy. *Invest Ophthalmol Vis Sci*. 2011; 52(11):7987–95. [PubMed: 21896851]
21. Girard MJ, Beotra MR, Chin KS, et al. In vivo 3-dimensional strain mapping of the optic nerve head following intraocular pressure lowering by trabeculectomy. *Ophthalmology*. 2016 In Press.
22. Sibony P, Kupersmith MJ, Honkanen R, Rohlf FJ, Torab-Parhiz A. Effects of lowering cerebrospinal fluid pressure on the shape of the peripapillary retina in intracranial hypertension. *Invest Ophthalmol Vis Sci*. 2014; 55(12):8223–31. [PubMed: 25406288]
23. Glassman AR, Melia M. Randomizing 1 eye or 2 eyes: a missed opportunity. *JAMA Ophthalmol*. 2015; 133(1):9–10. [PubMed: 25256889]
24. Murdoch IE, Morris SS, Cousens SN. People and eyes: statistical approaches in ophthalmology. *Br J Ophthalmol*. 1998; 82(8):971–3. [PubMed: 9828786]
25. Jonas JB, Nguyen XN, Gusek GC, Naumann GO. Parapapillary chorioretinal atrophy in normal and glaucoma eyes. I. Morphometric data. *Invest Ophthalmol Vis Sci*. 1989; 30(5):908–18. [PubMed: 2722447]
26. Hayashi K, Tomidokoro A, Lee KY, et al. Spectral-domain optical coherence tomography of beta-zone peripapillary atrophy: influence of myopia and glaucoma. *Invest Ophthalmol Vis Sci*. 2012; 53(3):1499–505. [PubMed: 22323471]
27. Xu L, Wang Y, Yang H, Jonas JB. Differences in parapapillary atrophy between glaucomatous and normal eyes: the Beijing Eye Study. *Am J Ophthalmol*. 2007; 144(4):541–6. [PubMed: 17651676]
28. Lamparter J, Russell RA, Zhu H, et al. The influence of intersubject variability in ocular anatomical variables on the mapping of retinal locations to the retinal nerve fiber layer and optic nerve head. *Invest Ophthalmol Vis Sci*. 2013; 54(9):6074–82. [PubMed: 23882689]
29. Teng CC, De Moraes CG, Prata TS, et al. The region of largest beta-zone parapapillary atrophy area predicts the location of most rapid visual field progression. *Ophthalmology*. 2011; 118(12):2409–13. [PubMed: 21885127]
30. Koh V, Tan C, Tan PT, et al. Myopic maculopathy and optic disc changes in highly myopic young Asian eyes and impact on visual acuity. *Am J Ophthalmol*. 2016; 164:69–79. [PubMed: 26850176]

31. Jonas JB, Wang N, Yang D, Ritch R, Panda-Jonas S. Facts and myths of cerebrospinal fluid pressure for the physiology of the eye. *Prog Retin Eye Res.* 2015; 46:67–83. [PubMed: 25619727]
32. Park HY, Lee KI, Lee K, Shin HY, Park CK. Torsion of the optic nerve head is a prominent feature of normal-tension glaucoma. *Invest Ophthalmol Vis Sci.* 2015; 56(1):156–63.
33. Samarawickrama C, Mitchell P, Tong L, et al. Myopia-related optic disc and retinal changes in adolescent children from Singapore. *Ophthalmology.* 2011; 118(10):2050–7. [PubMed: 21820741]
34. How AC, Tan GS, Chan YH, et al. Population prevalence of tilted and torted optic discs among an adult Chinese population in Singapore: the Tanjong Pagar Study. *Arch Ophthalmol.* 2009; 127(7): 894–9. [PubMed: 19597111]
35. Song BJ, Caprioli J. New directions in the treatment of normal tension glaucoma. *Indian J Ophthalmol.* 2014; 62(5):529–37. [PubMed: 24881596]
36. Apple DJ, Rabb MF, Walsh PM. Congenital anomalies of the optic disc. *Surv Ophthalmol.* 1982; 27(1):3–41. [PubMed: 6753203]
37. Kim TW, Kim M, Weinreb RN, Woo SJ, Park KH, Hwang JM. Optic disc change with incipient myopia of childhood. *Ophthalmology.* 2012; 119(1):21–6. e1–3. [PubMed: 21978594]
38. Thomas JG. The dynamics of small saccadic eye movements. *J Physiol.* 1969; 200(1):109–27. [PubMed: 5761933]
39. Bellezza AJ, Rintalan CJ, Thompson HW, Downs JC, Hart RT, Burgoyne CF. Deformation of the lamina cribrosa and anterior scleral canal wall in early experimental glaucoma. *Invest Ophthalmol Vis Sci.* 2003; 44(2):623–37. [PubMed: 12556392]
40. Lee EJ, Kim TW, Weinreb RN. Reversal of lamina cribrosa displacement and thickness after trabeculectomy in glaucoma. *Ophthalmology.* 2012; 119(7):1359–66. [PubMed: 22464141]
41. von Helmholtz, H. *Helmholtz's Treatise on Physiological Optics*, translated from the Third German Edition. Ithaca, NY: The Optical Society of America; 1924.
42. Friedman B. Mechanics of optic nerve traction on the retina during ocular rotation with special reference to retinal detachment. *Arch Ophthalmol.* 1941; 25(4):564–575.
43. Friedman B. Observations on entoptic phenomena. *Arch Ophthalmol.* 1942; 28(2):285–312.
44. Barr AE, Barbe MF. Pathophysiological tissue changes associated with repetitive movement: a review of the evidence. *Phys Ther.* 2002; 82(2):173–87. [PubMed: 11856068]
45. Snook SH, Vaillancourt DR, Ciriello VM, Webster BS. Psychophysical studies of repetitive wrist flexion and extension. *Ergonomics.* 1995; 38(7):1488–507. [PubMed: 7635136]
46. Wu CC, Kowler E. Timing of saccadic eye movements during visual search for multiple targets. *J Vis.* 2013; 13(11)
47. Robinson, DA. *Handbook of physiology, Section I: The nervous system.* Bethesda, MD: American Physiological Society; 1981. Control of eye movements.
48. Leclair-Visonneau L, Oudiette D, Gaymard B, Leu-Semenescu S, Arnulf I. Do the eyes scan dream images during rapid eye movement sleep? Evidence from the rapid eye movement sleep behaviour disorder model. *Brain.* 2010; 133(Pt 6):1737–46. [PubMed: 20478849]
49. David T, Smye S, James T, Dabbs T. Time-dependent stress and displacement of the eye wall tissue of the human eye. *Med Eng Phys.* 1997; 19(2):131–9. [PubMed: 9203147]
50. Demer JL, Dushyanth A. T2-weighted fast spin-echo magnetic resonance imaging of extraocular muscles. *J AAPOS.* 2011; 15(1):17–23. [PubMed: 21397801]

Biographies

Melinda Y. Chang, MD, is currently the Cooperman Fellow in Neuro-Ophthalmology at the combined Stein Eye Institute-Doheny Eye Institute at the University of California, Los Angeles (UCLA). She was the 2015-2016 Leonard Apt Fellow in Pediatric Ophthalmology at the Stein Eye Institute, and also completed ophthalmology residency at UCLA. Her research interests include the application of novel imaging techniques to disorders of the optic nerve and ocular motility, and the management of complex strabismus.



Joseph L. Demer, M.D., Ph.D. is Arthur Rosenbaum Professor, Chief of Pediatric Ophthalmology and Strabismus, and Professor of Neurology, at the David Geffen School of Medicine at UCLA. He directs the Ocular Motility Clinical Laboratory, and the EyeSTAR Program. Dr. Demer received the Friedenwald Award from ARVO, and a Recognition Award from Alcon Research Institute, for his work on biomechanics of extraocular muscles and orbital connective tissues. Dr. Demer is a gold fellow of ARVO.



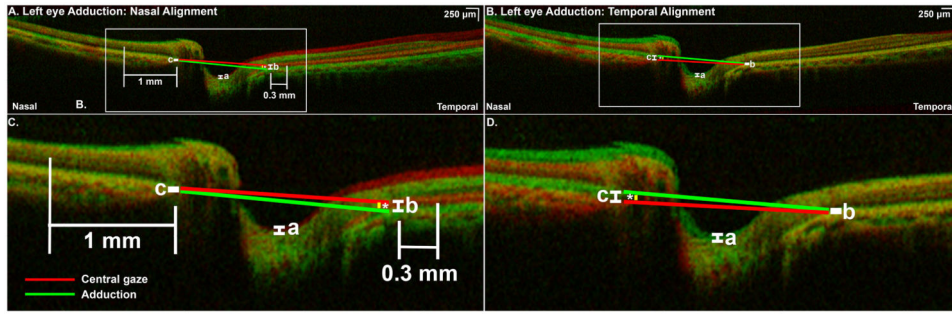


Fig. 1.
 A) Nasally superimposed optical coherence tomography (OCT) scans of a left eye in central gaze (red) and 30° adduction (green) demonstrating posterior displacement of optic cup and temporal peripapillary retinal pigment epithelium (tRPE) in adduction. B) Magnified view of rectangular peripapillary area shown in Fig. 1A. Optic cup displacement (OCD) was measured at maximum depth of the cup (a) and posterior shift of the tRPE at the temporal junction of the retinal pigment epithelium (RPE) and the optic nerve head (ONH, b). In this case, there was minimal displacement of the nasal peripapillary retinal pigment epithelium (nRPE), measured at the nasal junction of the ONH and RPE (c). Nasal choroidal thickness was measured 1 mm nasal to the junction of ONH and RPE; temporal choroidal thickness was measured 0.3 mm temporal to the junction of ONH and RPE. A line connecting the immediate nasal and temporal peripapillary RPE defined the ONH angle in central (red line) and eccentric gaze (green line). Change in ONH angle (*) was considered positive when the ONH was tilted temporally in eccentric gaze, as here. C) Superimposed OCTs of the same eye in the identical conditions as in Fig. 1A, aligned temporally rather than nasally. OCT in central gaze is shaded red and 30° adduction is shaded green. D) Magnified view of rectangular peripapillary area shown in Fig. 1C. Temporal alignment demonstrates relative anterior displacement of the optic cup in adduction (a), of the same magnitude but opposite in direction to OCD when the scans are aligned nasally. The relative anterior displacement of the nRPE (c) is equal in magnitude to the relative posterior displacement of the tRPE when nasal alignment is performed. The degree of ONH tilt (*) is unchanged when scans are aligned nasally or temporally.

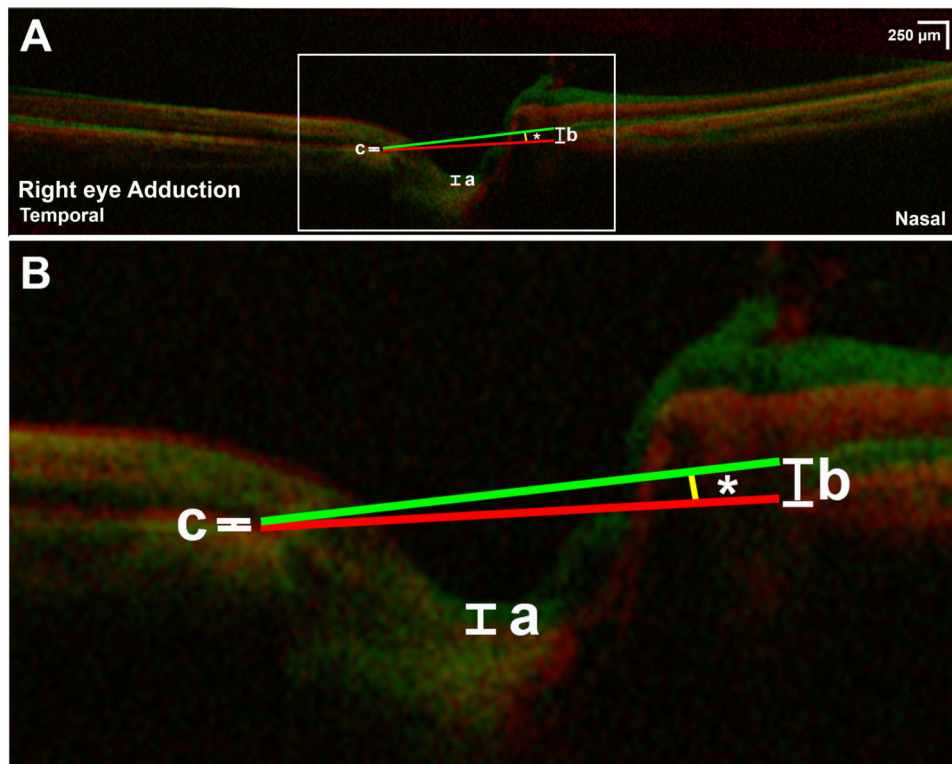


Fig. 2.

A) Superimposed optical coherence tomography of a right eye in central gaze (red) and 30° adduction (green). B) Magnified view of rectangular area in Fig 2A shows “nasal buckling,” sharp anterior angulation of the nasal peripapillary tissues adjacent to the optic nerve head (ONH) with associated anterior shift of the optic cup (a). Anterior shift of the nasal peripapillary RPE (nRPE) was measured at the junction of the nasal peripapillary RPE and ONH (b). There was minimal shift of the temporal peripapillary RPE (tRPE) in this case (c). The ONH tilted temporally by 5.3° in 30° adduction (*).

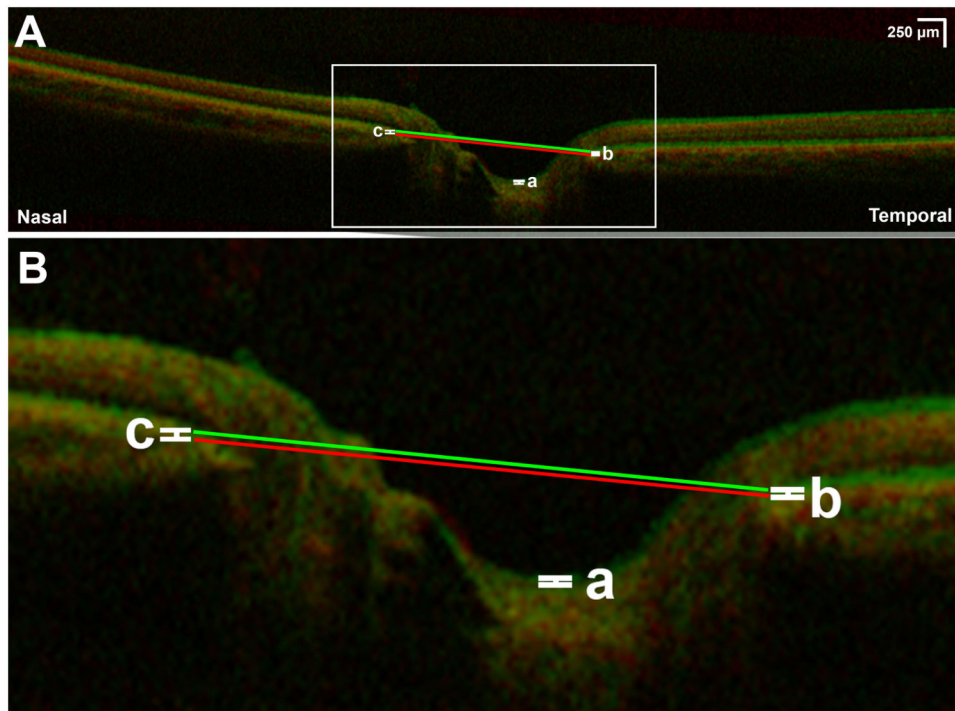


Fig. 3.

A) Superimposed optical coherence tomography of left eye demonstrating effect of 30° abduction (green) compared to central gaze (red). B) Magnification of rectangular area indicated in Fig 3A. There is minimal anterior displacement of the optic cup (a), temporal peripapillary retinal pigment epithelium (b), and nasal peripapillary retinal pigment epithelium (c). Lines defining optic nerve head angle in central gaze (red line) and abduction (green line) are parallel, indicating absence of angle change with 30° abduction.

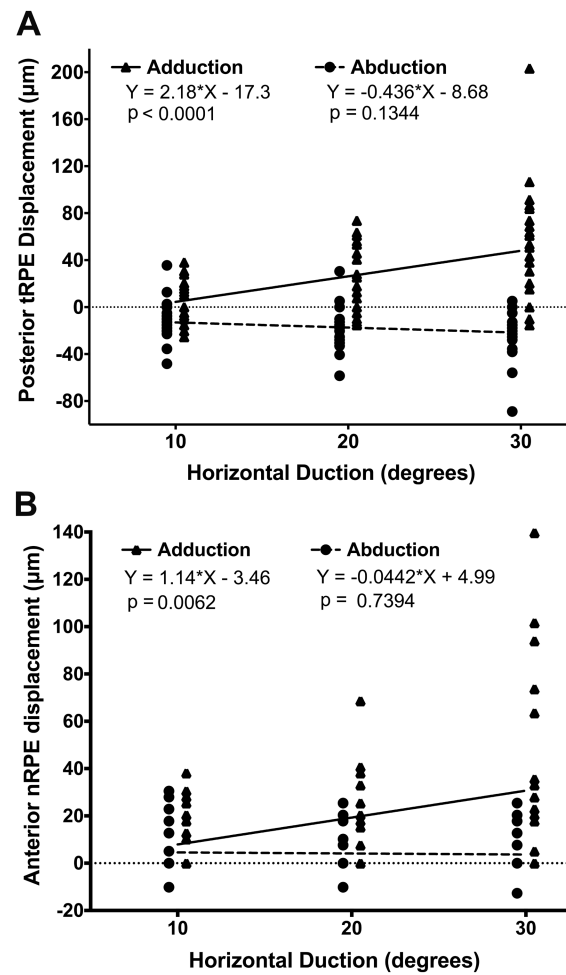


Fig. 4.
 A) Posterior displacement of temporal peripapillary RPE (tRPE) in horizontal duction.
 B) Anterior displacement of nasal peripapillary RPE (nRPE) in horizontal duction. Only adduction was associated with significant displacement by linear regression.

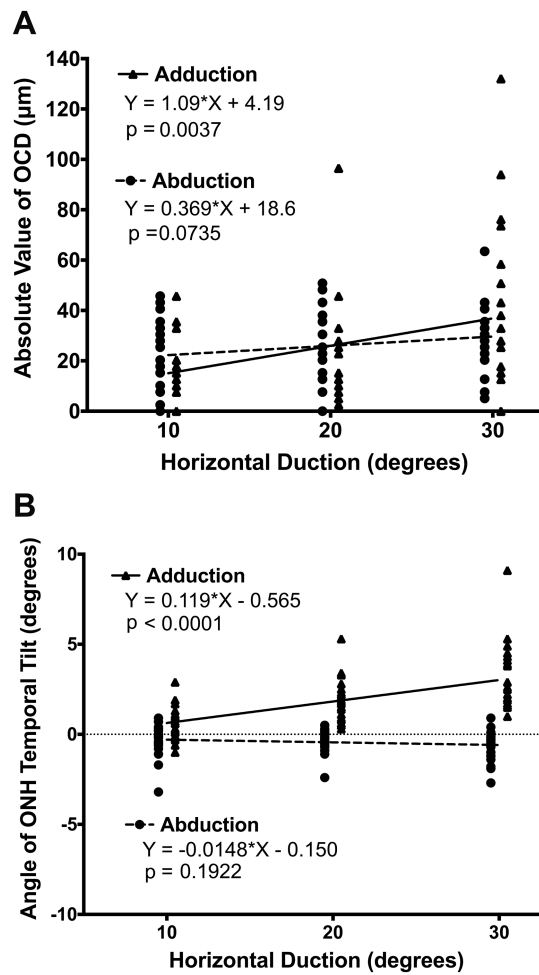


Fig. 5. A) Absolute optic cup displacement (OCD) vs. horizontal duction. B) Temporal tilt of optic nerve head (ONH) during horizontal duction. Adduction but not abduction was associated with significant OCD and tilting by linear regression.

Table 1
Mean Choroidal Thickness

	Nasal Thickness (μm , SEM)	Temporal Thickness (μm , SEM)
Central gaze	247 (10)	184 (9)
Repeat central gaze	254 (18) p=0.51	192 (15) p = 0.18
Adduction		
10°	232 (10)*	175 (8) [†]
20°	232 (11)*	171 (8) [†]
30°	232 (11)*	166 (8) [†]
	*P < 0.0005	[†] P < 0.03
Abduction		
10°	235 (10)**	174 (8) [‡]
20°	230 (10)**	167 (8) [‡]
30°	228 (10)**	166 (6) [‡]
	**P < 0.002	[‡] P < 0.02

Choroidal thickness in central gaze, repeat central gaze, and eccentric gazes. SEM - standard error of mean.